IEEE Access
Multidisciplinary | Rapid Review | Open Access Journal

Received August 20, 2019, accepted September 10, 2019, date of publication September 13, 2019,
date of current version September 30, 2019.

Digital Object Identifier 10.1109/ACCESS.2019.2941262

High Spectral Resolution Raman Measurements Using Light-Emitting Diode as Excitation Based on Weighted Spectral Reconstruction Method

SHUO CHEN[1,3], (Member, IEEE), MIXING LIU[1], JING LIU[2], LINGMIN KONG[1], WENBIN XU[2], GANG HOU[4], LIPING XIE[1], AND XIAOYU CUI[1,3]

[1]College of Medicine and Biological Information Engineering, Northeastern University, Shenyang 110819, China
[2]Science and Technology on Optical Radiation Laboratory, Beijing 110854, China
[3]Key Laboratory of Data Analytics and Optimization for Smart Industry (Northeastern University), Ministry of Education, Shenyang 110819, China
[4]Institute of Respiratory Disease, The First Hospital of China Medical University, Shenyang 110004, China

Corresponding author: Xiaoyu Cui (cuixy@bmie.neu.edu.cn)

This work was supported in part by the National Natural Science Foundation of China under Grant 61605025 and Grant 81501556, in part by the Fund for Innovative Research Groups of the National Natural Science Foundation of China under Grant 71621061, in part by the Science and Technology Foundation of National Defense Key Laboratory under Grant 61424080209, in part by the Program for Innovation Talents in Universities of Liaoning Province under Grant LR2016031, in part by the Ningbo Natural Science Foundation under Grant 2018A610365, in part by the Fundamental Research Funds for the Central Universities under Grant N171902001, Grant N171904006, and Grant N180719020, and in part by the 111 Project under Grant B16009.

ABSTRACT Raman spectroscopy is a spectroscopic technique that can provide rich biochemical information about the sample through the inelastic scattering between monochromatic light and molecular vibrations, thus a narrow bandwidth and costly laser is typically required. Although the replacement of laser to light-emitting diode (LED) can reduce the cost significantly, spectral resolution degrades seriously and a large amount of Raman fingerprint information is lost due to the overlaps of Raman peaks. In this study, a weighted spectral reconstruction method was developed to retrieve high quality Raman spectrum from the Raman measurements using LED as the excitation, in which the LED based Raman measurements were numerically synthesized from the Raman spectra acquired by the conventional laser-based Raman spectroscopy systems. The proposed weighted spectral reconstruction method was numerically test on the synthesized LED based Raman measurements from 25 agar phantoms, 50 blood serum samples, and 56 cell samples, respectively. According to the results, the restored Raman spectra are in excellent agreement with the conventional Raman spectra, and the differences are always less than 2% in all test samples. Therefore, Raman measurements using LED as excitation combined with weighted spectral reconstruction method demonstrate significant potential in accurate and high spectral resolution Raman measurements, which promotes a cost-effective Raman setup while preserve the most important spectral and biochemical information.

INDEX TERMS Raman spectroscopy, spectral restoration, light-emitting diode, weighted spectral reconstruction.

I. INTRODUCTION

Raman spectroscopy is a non-invasive vibrational spectroscopic technique and can provide quantitative fingerprint information about molecular vibrations, which relies on the inelastic scattering (i.e. Raman scattering) between the monochromatic photons and molecules [1]. Rich biochemical information about the sample can be detected based on the gain and loss of photon energy [2], thus Raman spectroscopy has been widely used to study the chemical composition and structure of molecules from fundamental research to industrial applications, including material science [3], chemistry [4], geology [5], biology [6], medicine [7], etc. For conventional Raman spectroscopy systems, narrow bandwidth and costly lasers in the ultraviolet, visible or infrared region are typically employed as excitation source to provide the required monochromatic light, thus the applications of Raman spectroscopy technique are often restricted by its high

The associate editor coordinating the review of this manuscript and approving it for publication was Jiajie Fan.

cost and low portability [8]. Light-emitting diode (LED), a kind of light source widely available in all spectral ranges (from deep UV to IR), is inexpensive, long life-time, low power consumption, and small in size, thus offer the possibility of building low cost and portable Raman spectroscopy system. However, its broad bandwidth can cause overlaps of those sharp Raman peaks, hence spectral resolution can degrade seriously and a large amount of Raman fingerprint information is lost.

Over the past decades, several attempts have been made to use LED as the excitation source in Raman spectroscopy system and several advanced methods have been developed to overcome the above limitations. Schmidt and Kiefer [9] demonstrated a straightforward method to obtain the Raman spectra by using LED with the output power of 650mw and the full width half maximum (FWHM) of approximately 15nm, in which the laser-line filter was employed to extract the narrow-band radiation from broadband LED. Renata and Kiefer [10] further tuned the spectral profile by shifting the bandpass filter by 3° to generate tunable narrow-band radiation, thus Raman spectra at two different excitation wavelengths can be obtained and the fluorescence-free Raman spectrum can subsequently be reconstructed. However, for both of those two methods, the spectral resolution in the ultraviolet spectral range could be much worse compared to that in the infrared spectral range, because the resulting spectral profile should only be determined by the configuration of the bandpass filter and the transmission window of the bandpass filter is typically restrict to the order of 1nm. In addition, only a small portion of LED power can reach onto the sample, thus a high-power LED is typically required to produce sufficient Raman scattering photons. In contrast, Greer *et al.* [11] developed a totally different approach and made full usage of the broad bandwidth of the LED, thus only a 3mW broadband (FWHM $\sim$ 40nm) LED was employed to collect sufficient Raman signal. The broadband radiation was spatially dispersed in a line focus by a pair of diffraction gratings and an achromatic lens, and the Raman spectra excited at different wavelengths reached onto the different rows of the CCD detector and finally recombined to a single Raman spectrum. However, the disadvantage might be the complex experimental setup and sophisticated numerical algorithms to reconstruct the final Raman spectrum with optimal spectral resolution.

Spectral reconstruction from narrow-band measurements [12] might be a potential way to achieve high spectral resolution Raman measurements with LED excitation. This method was originally developed for fast Raman spectroscopic imaging, in which high spatial and spectral resolution Raman measurements can be reconstructed from a few narrow-band images [13]. In such a method, those narrow-band images are taken by collecting the Raman scattering photons after passing through several specific filters. The core of spectral reconstruction method is that the most important Raman spectral information is compressed into narrow-band measurements due to its sparsity, and high spectral resolution Raman spectrum at each pixel can subsequently be retrieved by supervised learning spectral reconstruction algorithms. Although the spectral resolution degrades seriously by collecting narrow-band measurements instead of intensities at each wavelengths, the spectral reconstruction algorithms are insensitive to the degradation of spectral resolution because of the prior knowledge extracted from the relationship between the high spectral resolution Raman spectra and the narrow-band measurements in the training dataset. Our previous studies [14]–[16] have theoretically and experimentally demonstrate the feasibility of accurate Raman reconstruction from the corresponding narrow-band measurements. For the LED based Raman measurements, the Raman spectral resolution similarly degrades due to its non-monochromatic property, thus spectral reconstruction based method is expected and should be feasible to restore high spectral resolution Raman spectra from LED based Raman measurements.

In this study, a weighted spectral reconstruction method was developed and investigated to reconstruct high spectral resolution Raman spectra from the Raman measurements using LED as the excitation, which makes the full usage of the broad bandwidth of the LED. The proposed method was theoretically evaluated by the synthesized LED based Raman measurements from 25 agar phantoms, 50 blood serum samples, and 56 cells samples. The results demonstrated that high spectral resolution Raman measurements can be extracted from the Raman measurements excited by broadband LED. Thus, the methods described in this paper can be applicable to a portable and cost-effective Raman spectroscopy system or even Raman spectroscopic imaging setup.

II. CONVENTIONAL RAMAN MEASUREMENTS AND SYNTHESIS OF LED BASED RAMAN MEASUREMENTS

A. SAMPLE PREPARATION AND CONVENTIONAL RAMAN MEASUREMENTS

1) PHANTOMS

Potassium formate (294454, Sigma-Aldrich, US) and urea (V3171, Promega corporation, US) were dissolved in distilled water and then mixed with 1.5% agar solution (PC0701, Vivantis Technologies, US). In total, 25 agar phantoms were made with different concentration, in which the concentrations for both potassium formate and urea in the final mixture were 0.25 M, 0.5 M, 1 M, 1.5 M, and 2 M respectively. The micro-Raman spectroscopy system (innoRam-785S, B&W TEK, US) was used to collect the Raman spectra from the agar phantoms. The Raman signals were excited by a 785nm laser and measured over a range from 600 cm^{-1} to 1800 cm^{-1} with the spectral resolution of 4 cm^{-1}. The exposure time for the Raman measurements of phantoms was 10s, and each Raman spectrum was accumulated for 30 times.

2) BLOOD SERUM SAMPLES

The blood serum samples were collected from 50 nasopharyngeal cancer patients in Fujian Tumor hospital, Fuzhou, China. Those blood serum samples were centrifuged at

2,000 rpm for 15 minutes for blood cells removal and mixed with silver colloidal nanoparticles, and then kept at 4°C for two hours before taking the Raman measurements. The confocal Raman microscope (inVia, Renishaw, UK) was used to collect the surface-enhanced Raman scattering (SERS) measurements from those blood serum samples. The Raman signals were excited by a 785nm laser and measured over a range from 600 cm^{-1} to 1800 cm^{-1} with the spectral resolution of 2 cm^{-1}. The exposure time for the Raman measurements of blood serum samples was 10s, and each spectrum was accumulated only once.

3) CELLS

Two different types of cells were cultured and measured, i.e. the renal cells (Caki-2 cells) and leukemia cells (K562 cells). Those cells were washed twice by phosphate-buffered saline (PBS) to alleviate the significant fluorescence background from the culture media for optimal Raman signal acquisition. In total, 56 Raman spectra were taken from those cell samples, in which both types of cells contributed 28 Raman measurements respectively. The confocal Raman microscope (inVia, Renishaw, UK) was used to collect the Raman spectra from those cell samples. The Raman signals were excited by a 785nm laser and measured over a range from 600 cm^{-1} to 1800 cm^{-1} with the spectral resolution of 2 cm^{-1}. The exposure time for the Raman measurements of cells was 10s, and each Raman spectrum was accumulated for 6 times.

B. SYNTHESIS OF LED BASED RAMAN MEASUREMENTS

The synthesis of LED based Raman measurements was implemented based on the assumption that the Raman shifts are always consistent when using different excitation wavelengths and the LED can be equivalent to the combination of multiple narrow-band lasers with different wavelengths when exciting Raman signals. Since the fluorescence background should negligibly change when the excitation tuned within a small wavelength range [17], the fluorescence background signals were assumed to be unchanged when replacing narrow-band lasers with LEDs. Thus, by employing LEDs as the excitation, the changes of the narrow-band measurements are mainly contributed by the distorted Raman signal other than fluorescence background, in which the fluorescence background can be ignored in this study and was removed from the original Raman measurements by using the fifth-order polynomial fitting before synthesizing the LED based Raman measurements. More specifically, the unchangeable fluorescence background has little impact on the spectral reconstruction, and the slight degradation (less than 0.9%) of the spectral reconstruction accuracies between the narrow-band measurements in the presence and absence of fluorescence background has already been investigated in our previous studies [16]–[18], thus the fluorescence background was not considered in order to simplify and focus on the spectral reconstruction problems induced by the LEDs. The LED based Raman measurements can be derived from the conventional Raman spectrum after fluorescence background removal according to (1).

$$\lambda_R = \frac{\lambda_0}{1 - \lambda_0} \Delta w \tag{1}$$

where λ_0 and λ_R refer to the excitation wavelength and Raman wavelength with the unit of cm respectively, and Δw refers to the Raman shift with the unit of cm^{-1}. Thus, the LED based Raman signal can be numerically simulated based on the known excitation wavelength range of the LED and the known Raman spectrum, in which the conventional Raman spectrum after fluorescence background removal was treated as the input known Raman spectrum. Since discretization has to be implemented during the numerical simulation, the step size of the excitation wavelengths was set to 0.01nm, in which less than 0.02% difference was always observed when using a smaller step size, i.e. 0.001nm. LEDs with different bandwidths from 5nm to 50nm were used to verify the feasibility of acquiring high spectral resolution Raman measurements with LEDs and to investigate the impact of LED bandwidths on the spectral reconstruction accuracy.

III. WEIGHTED SPECTRAL RECONSTRUCTION METHOD

In this study, weighted spectral reconstruction method was developed and employed to retrieve high spectral resolution Raman measurements from synthesized LED based Raman measurements. The weighted spectral reconstruction method consists of two steps, i.e. the weight calculation step and weighted Wiener estimation step, as show in Figure 1.

In the weight calculation step, reconstructed Raman spectra with high spectral resolution is restored from narrow-band measurements by traditional Wiener estimation [19], [20], in which the narrow-band measurements are numerically generated by the inner product between synthesized LED based Raman measurements and non-negative principal components (PCs) based filters. Those non-negative PCs based filters are derived by using a invertible linear transform of characteristic spectra, in which those characteristic spectra are equivalent to the orthogonal vectors from a principal component analysis of the conventional Raman measurements. More specifically, the non-negative PCs based filter sets can be obtained by parameterized adding a multiple of the first characteristic spectrum to the others, thus the optimal compression properties of the PCA scheme can be maintained in such parameterized design space. The final set of non-negative PCs based filters is found by solving a linearly constrained nonlinear programming problem, which gives minimum noise amplification. In short, the non-negative PCs based filters are derived by a published method [21] based on principal component analysis (PCA) of the conventional Raman spectra and can optimally compress most important spectral information about the Raman spectral reconstruction into the narrow-band measurements. The traditional Wiener estimation is a supervised learning method and typically involves two stages, i.e. the training stage and the test stage. In the training stage for weight calculation in this study, Wiener matrix W is created to learn supervised from the

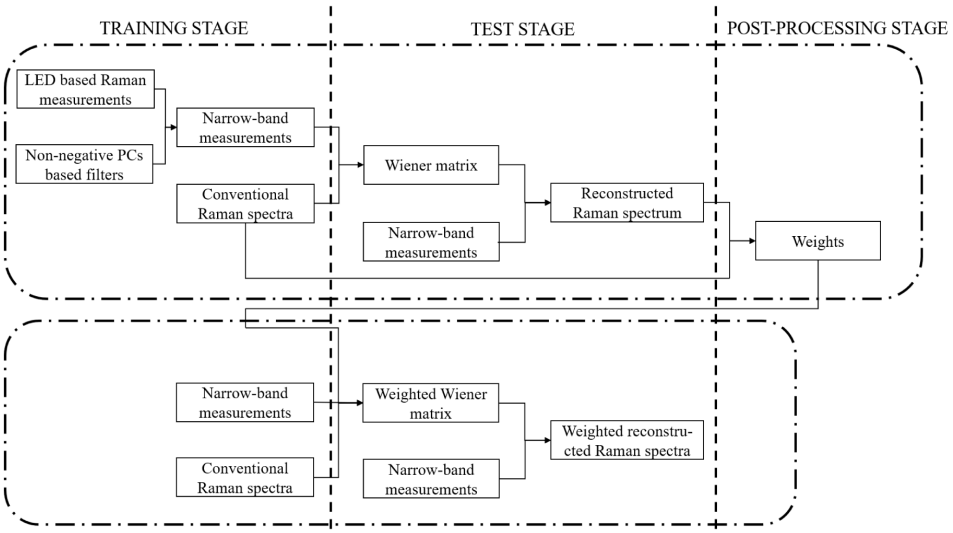

FIGURE 1. General procedure for weighted spectral reconstruction.

training dataset according to (2), in which the model between the conventional high spectral resolution Raman spectra r and the corresponding LED based narrow-band measurements m in the calibration dataset can be built.

$$W = E\left(rm^T\right)\left[E(mm^T)\right]^{-1} \tag{2}$$

where E() is the ensemble average, the superscript 'T' is matrix transpose, and the superscript '−1' is matrix inverse. In the test stage, the reconstructed Raman spectra R with high spectral resolution can be recovered from the corresponding LED based Raman measurements N in the test dataset according to (3).

$$R = WN \tag{3}$$

Finally, the weights w_i for each narrow-band measurement in the training dataset can be derived based on the differences between the conventional Raman spectra and the reconstructed Raman spectra according to (4), i.e. larger difference corresponds to lower weight.

$$w_i = \frac{d_i^{-1}}{\sum_{i=1}^{n} d_i^{-1}} \tag{4}$$

where d_i is the summation of the absolute differences at each wavelengths between the reconstructed Raman spectrum and the i-th conventional Raman spectrum in the training dataset, and n is total number of samples in the training dataset.

In the weighted Wiener estimation step, the weights derived in the above step are integrated with traditional Wiener estimation according to (5), in which the weighted Wiener matrix are mostly contributed by the training data with higher similarity to the test data. By such method, more precise model between reference Raman spectra and their corresponding LED based narrow-band measurements can be built for each test samples, thus the spectral reconstruction accuracy is expected to be improved significantly.

$$\bar{W} = \sum_{i=1}^{n} w_i r_i m_i^T \sum_{i=1}^{n} (w_i r_i m_i^T)^{-1} \tag{5}$$

where $\bar{W}$ refers to the weighted Wiener matrix, and w_i, r_i, and m_i refer to the weight, conventional Raman spectrum and narrow-band measurements of the i-th set of training data respectively. The final weighted reconstructed Raman spectrum for each test sample is calculated by the inner production of the corresponding weighted Wiener matrix and narrow-band measurements of the test sample. The mean relative root means square error (RMSE) [22] between the weighted reconstructed Raman spectra and the reference Raman spectra is served as the criterion to evaluate the performance of the proposed weighted spectral reconstruction method. Furthermore, since the proposed weighted wiener estimation is a supervised learning method in nature, leave-one-out method is used for cross-validation to test all samples in an unbiased way.

IV. RESULTS AND DISCUSSIONS

The comparison of the conventional Raman spectra and the synthesized LED based Raman spectra with bandwidth of 5nm, 10nm and 50nm is shown in Figure 2. It is obvious that the overlaps and distortions of the Raman peaks occur as we expected due to the replacement of narrow-band lasers to LEDs, and those overlaps and distortions are much more serious when larger bandwidth of LEDs is employed as the excitation. In addition, the overlaps and distortions of Raman peaks become more serious when there are more Raman peaks and more complex Raman spectral shapes within the conventional Raman spectra. Thus, it is expected that the recovery of high spectral resolution Raman spectra from LED based Raman should be more difficult with the increment of LED bandwidth and Raman spectral complexity.

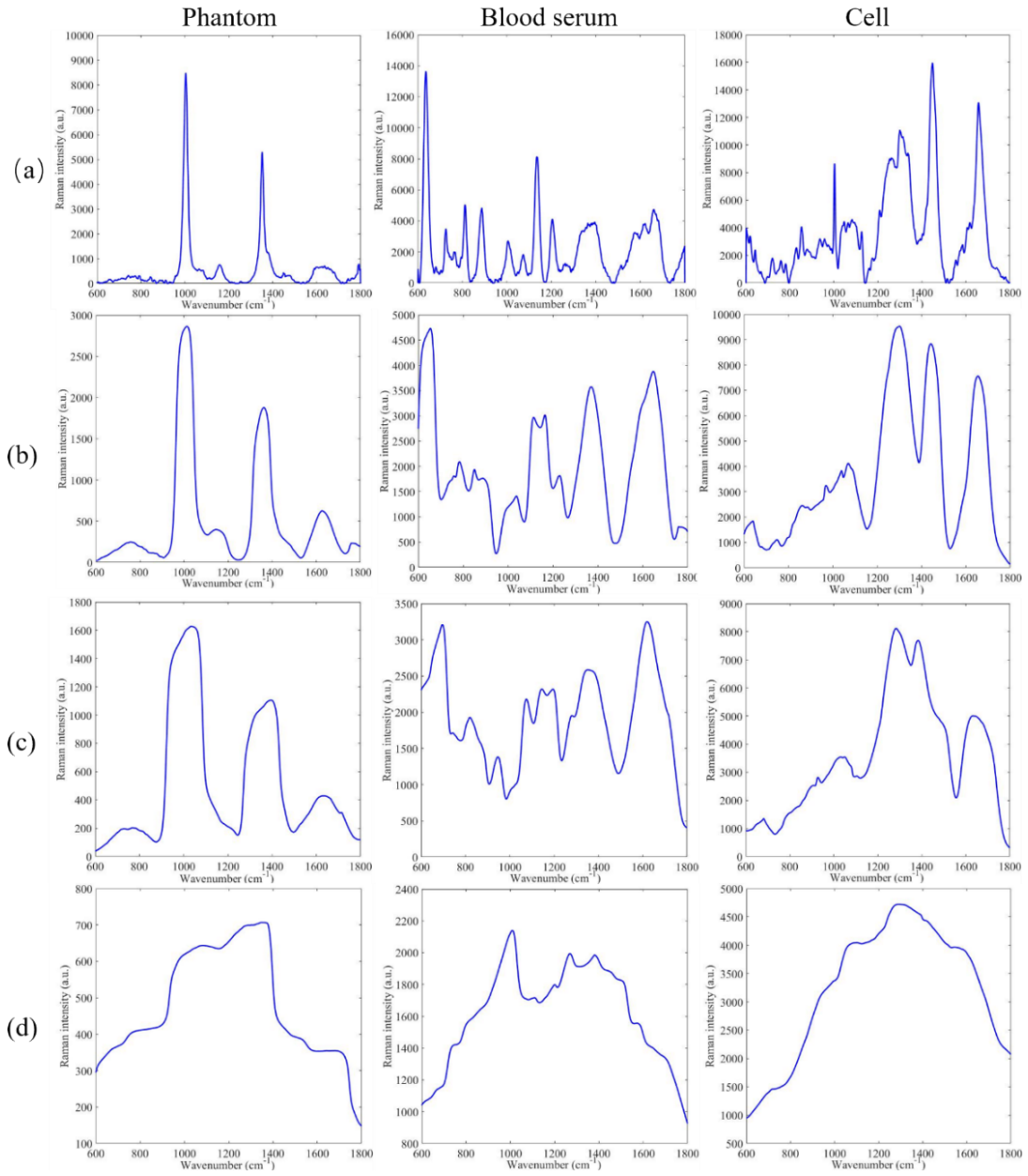

FIGURE 2. Comparison of the (a) conventional Raman spectra of phantom, blood serum and cell samples, and the corresponding synthesized LED based Raman spectra with bandwidths of (b) 5nm, (c) 10nm, and (d) 50nm.

TABLE 1. The mean relative RMSEs between the reconstructed Raman spectra from synthesized LED based Raman measurements and the corresponding conventional Raman spectra using different bandwidths and numbers of non-negative PCs based filter for agar phantom samples.

Number of filters	LED Bandwidth (nm)					
	5	10	20	30	40	50
3	6.94×10^{-3}	7.61×10^{-3}	8.15×10^{-3}	8.11×10^{-3}	8.31×10^{-3}	8.20×10^{-3}
4	5.57×10^{-3}	$\mathbf{5.81\times10^{-3}}$	6.28×10^{-3}	7.33×10^{-3}	6.21×10^{-3}	6.33×10^{-3}
5	6.52×10^{-3}	6.55×10^{-3}	6.49×10^{-3}	6.00×10^{-3}	1.03×10^{-2}	4.92×10^{-3}
6	7.07×10^{-3}	7.73×10^{-3}	6.83×10^{-3}	6.97×10^{-3}	9.84×10^{-3}	5.88×10^{-3}

For agar phantoms, the mean relative RMSEs between the reconstructed Raman spectra from synthesized LED based Raman measurements and the corresponding conventional Raman spectra are shown in Table 1, in which different filter numbers ranged from 3 to 6 and different bandwidths ranged from 5nm to 50nm are investigated. It can be found

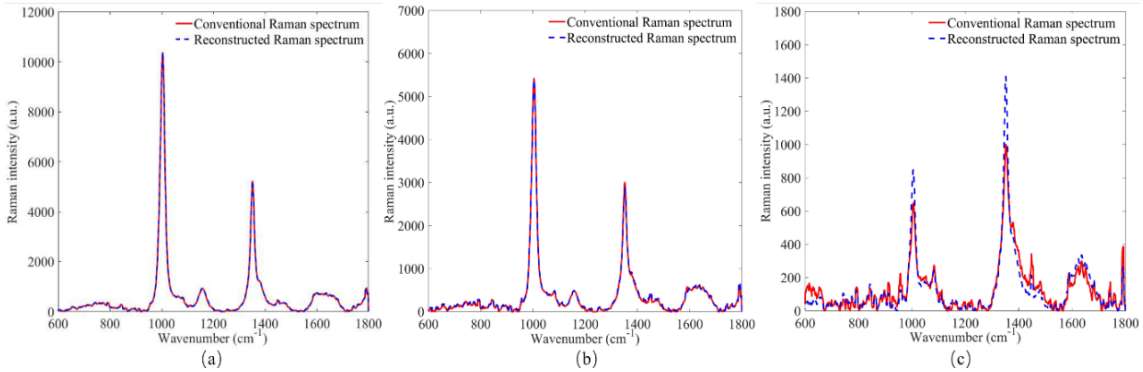

FIGURE 3. Comparison between the conventional Raman spectra and reconstructed Raman spectra from synthesized LED based Raman measurements in the (a) best case, (b) typical case and (c) worst case for agar phantom samples. Note that the bandwidth of LED is 10nm and the number of non-negative PCs based filter is 4.

TABLE 2. The mean relative RMSEs between the reconstructed Raman spectra from synthesized LED based Raman measurements and the corresponding conventional Raman spectra using different bandwidths and numbers of non-negative PCs based filter for blood serum samples.

Number of filters	LED Bandwidth (nm)					
	5	10	20	30	40	50
3	1.51×10^{-2}	1.82×10^{-2}	1.81×10^{-2}	1.84×10^{-2}	1.87×10^{-2}	1.84×10^{-2}
4	1.39×10^{-2}	1.52×10^{-2}	1.66×10^{-2}	1.68×10^{-2}	1.49×10^{-2}	1.46×10^{-2}
5	1.31×10^{-2}	1.42×10^{-2}	1.60×10^{-2}	1.46×10^{-2}	1.48×10^{-2}	1.41×10^{-2}
6	1.25×10^{-2}	1.41×10^{-2}	1.46×10^{-2}	1.38×10^{-2}	1.41×10^{-2}	1.38×10^{-2}
7	1.25×10^{-2}	1.37×10^{-2}	1.42×10^{-2}	1.35×10^{-2}	1.34×10^{-2}	1.34×10^{-2}
8	1.20×10^{-2}	1.31×10^{-2}	1.40×10^{-2}	1.28×10^{-2}	1.29×10^{-2}	1.31×10^{-2}
9	1.19×10^{-2}	1.29×10^{-2}	1.33×10^{-2}	1.27×10^{-2}	1.24×10^{-2}	1.30×10^{-2}
10	1.24×10^{-2}	1.32×10^{-2}	1.32×10^{-2}	1.24×10^{-2}	1.25×10^{-2}	1.21×10^{-2}
11	1.24×10^{-2}	1.29×10^{-2}	1.27×10^{-2}	1.24×10^{-2}	1.29×10^{-2}	1.24×10^{-2}
12	1.24×10^{-2}	1.29×10^{-2}	1.23×10^{-2}	1.24×10^{-2}	1.23×10^{-2}	1.19×10^{-2}
13	1.25×10^{-2}	1.25×10^{-2}	1.29×10^{-2}	1.26×10^{-2}	1.21×10^{-2}	1.21×10^{-2}
14	1.22×10^{-2}	$\mathbf{1.22\times10^{-2}}$	1.29×10^{-2}	1.24×10^{-2}	1.17×10^{-2}	1.20×10^{-2}
15	1.23×10^{-2}	1.23×10^{-2}	1.28×10^{-2}	1.19×10^{-2}	1.16×10^{-2}	1.22×10^{-2}

in Table 1 that the mean relative RMSEs typically follows a first decreasing and then increasing trend with the increased number of non-negative PCs based filters, when the LEDs bandwidth is fixed. Although more filters can extract more spectral information from the LED based Raman spectra, more redundant information such as noise can be acquired as well when the filter number is more than expected, thus the optimization of filter number is critical for an optimal spectral reconstruction. Based on the results in Table 1, the optimal number of filters should be 4 in most cases for agar phantom samples. In addition, the LED bandwidth provides a dominant impact on the spectral reconstruction accuracy when the number of filters is small, in which larger bandwidth usually lead to worse mean relative RMSEs. Since the LED has to be existed in real-world practical applications other than those numerically simulated non-negative PCs based filters, the choice of LED bandwidth should be based on the compromise between the availability of the LED bandwidth and spectral reconstruction accuracy. Take 4 non-negative PCs based filters and 10nm LED bandwidth as an example, the mean relative RMSE is 5.81×10^{-3}, and the comparisons between the conventional Raman spectrum and reconstructed Raman spectra from synthesized LED based Raman measurements are shown in Figure 3. The relative RMSEs in the best, typical and worst cases are 1.11×10^{-3}, 5.41×10^{-3}, and 5.79×10^{-2}, respectively. The best and worst cases refer to the reconstructed Raman spectra with the minimum and maximum relative RMSEs respectively, and the typical case refers to the reconstructed Raman spectrum with the relative RMSE closest to the mean relative RMSEs.

For blood serum samples, the mean relative RMSEs between the reconstructed Raman spectra from synthesized LED based Raman measurements and the corresponding conventional Raman spectra are shown in Table 2, in which different filter numbers range from 3 to 15 and different bandwidths range from 5nm to 50nm are investigated. It can

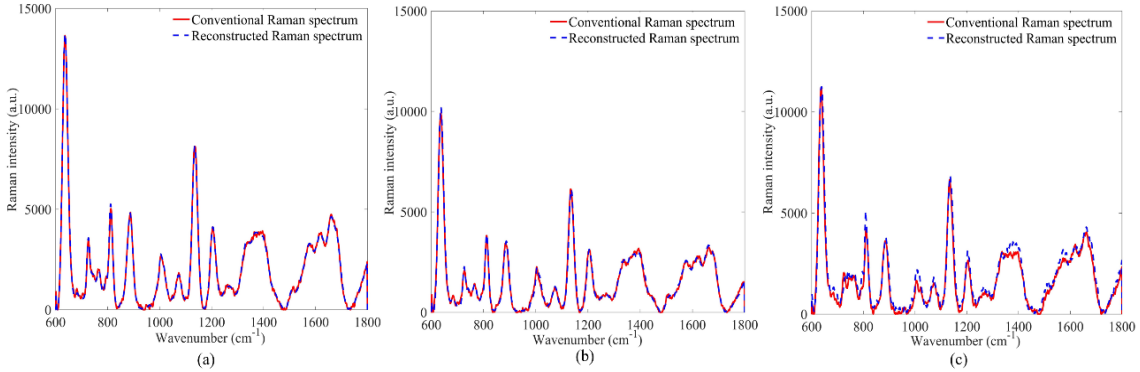

FIGURE 4. Comparison between the conventional Raman spectra and reconstructed Raman spectra from synthesized LED based Raman measurements in the (a) best case, (b) typical case, and (c) worst case for blood serum samples. Note that the bandwidth of LED is 10nm and the number of non-negative PCs based filters is 14.

TABLE 3. The mean relative RMSEs between the reconstructed Raman spectra from synthesized LED based Raman measurements and the corresponding conventional Raman spectra using different Bandwidths and numbers of non-negative PCs based filter for cell samples.

Number of filters	LED Bandwidth (nm)					
	5	10	20	30	40	50
3	2.44×10^{-2}	2.54×10^{-2}	2.84×10^{-2}	3.62×10^{-2}	3.27×10^{-2}	3.99×10^{-2}
4	2.18×10^{-2}	2.44×10^{-2}	2.60×10^{-2}	2.48×10^{-2}	2.55×10^{-2}	2.62×10^{-2}
5	2.27×10^{-2}	2.14×10^{-2}	2.53×10^{-2}	2.30×10^{-2}	2.34×10^{-2}	2.49×10^{-2}
6	2.01×10^{-2}	2.09×10^{-2}	2.40×10^{-2}	2.14×10^{-2}	2.17×10^{-2}	2.14×10^{-2}
7	1.73×10^{-2}	1.82×10^{-2}	1.93×10^{-2}	1.86×10^{-2}	1.86×10^{-2}	1.93×10^{-2}
8	1.78×10^{-2}	1.88×10^{-2}	1.87×10^{-2}	1.84×10^{-2}	1.80×10^{-2}	1.97×10^{-2}
9	1.88×10^{-2}	1.87×10^{-2}	1.91×10^{-2}	1.82×10^{-2}	1.89×10^{-2}	2.00×10^{-2}
10	1.83×10^{-2}	1.90×10^{-2}	1.85×10^{-2}	1.77×10^{-2}	1.93×10^{-2}	1.84×10^{-2}
11	1.88×10^{-2}	1.75×10^{-2}	1.90×10^{-2}	1.87×10^{-2}	1.88×10^{-2}	1.91×10^{-2}
12	1.73×10^{-2}	1.76×10^{-2}	1.91×10^{-2}	1.77×10^{-2}	1.77×10-2	1.91×10^{-2}
13	1.71×10^{-2}	1.70×10^{-2}	1.87×10^{-2}	1.77×10^{-2}	1.69×10^{-2}	1.91×10^{-2}
14	1.65×10^{-2}	$\mathbf{1.67\times10^{-2}}$	1.89×10^{-2}	1.76×10^{-2}	1.67×10^{-2}	1.85×10^{-2}
15	1.62×10^{-2}	1.67×10^{-2}	1.79×10^{-2}	1.72×10^{-2}	1.69×10^{-2}	1.83×10^{-2}

be found in Table 2 that the trends for blood serum samples among spectral reconstruction accuracy, number of non-negative PCs based filters and LED bandwidth are similar to that observed in the above agar phantoms. However, in general, the spectral reconstruction accuracies for blood serum samples are much lower compared to that for phantoms, and larger number of non-negative PCs based filters is required to achieve an optimal spectral reconstruction. This could be attributed to the fact that the blood serum SERS spectra contains more Raman peaks and fingerprint spectral information, thus the overlaps of the Raman peaks should be more serious when inducing LED as the excitation. Take 14 non-negative PCs based filters and 10nm LED bandwidth as an example, the mean relative RMSE is 1.22×10^{-2}, and the comparisons between the conventional Raman spectrum and reconstructed Raman spectra from synthesized LED based Raman measurements are shown in Figure 4. The relative RMSEs in the best, typical and worst cases are 7.10×10^{-3}, 1.22×10^{-2}, and 2.71×10^{-2}, respectively.

For cell samples, the mean relative RMSEs between the reconstructed Raman spectra from synthesized LED based Raman measurements and the corresponding conventional Raman spectra are shown in Table 3, in which different filter numbers range from 3 to 15 and different bandwidths range from 5nm to 50nm are investigated. It can be found in Table 3 that the trends for cell samples among spectral reconstruction accuracy, number of non-negative PCs based filters and LED bandwidth follow the similar trends of the above agar phantoms and blood serum samples. However, in general, the spectral reconstruction accuracies of the cell samples are the lowest among three different types of samples, which is due to the largest amount of Raman peaks and most complex Raman fingerprint information within the cell Raman spectra. Take 14 non-negative PCs based filters

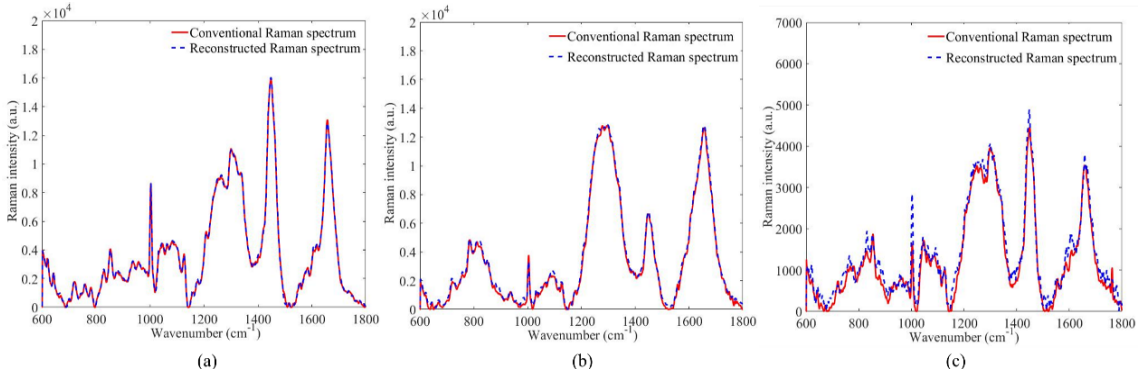

FIGURE 5. Comparison between the conventional Raman spectra and reconstructed Raman spectra from synthesized LED based Raman measurements in the (a) best case, (b) typical case, and (c) worst case for cell samples. Note that the bandwidth of LED is 10nm and the number of non-negative PCs based filters is 14.

and 10nm LED bandwidth as an example, the mean relative RMSE is 1.67×10^{-2}, and the comparisons between the conventional Raman spectrum and reconstructed Raman spectra from synthesized LED based Raman measurements are shown in Figure 5. The relative RMSEs in the best, typical and worst cases are 7.82×10^{-3}, 1.67×10^{-2}, and 4.98×10^{-2}, respectively.

In addition, the traditional Wiener estimation method alone was test on the LED based Raman measurements, however, much worse results were found. Take 10nm LED bandwidth as example, the mean relative RMSEs for the optimal number of non-negative PCs based filters are 6.50×10^{-3}, 1.59×10^{-2} and 2.23×10^{-2} for phantoms, blood serum samples and leukemia cells, respectively. Thus, compared with weighted Wiener estimation, the degradations of the spectral reconstruction accuracy are approximately 11.9%, 30.3% and 33.5% for phantoms, blood serum samples and leukemia cells, respectively. The results are much worse compared with the weighted spectral reconstruction method, especially when the complexity of the Raman spectral shape is higher. The reason is that the proposed weighted Wiener estimation method further considers the similarity between the calibration dataset and the test dataset, in which the training sample with higher similarity to the test sample contributes more when creating Wiener matrix, thus the Wiener matrix is optimized for each test sample and the spectral reconstruction accuracy can be improved.

In order to mimic the real situation more accurately, Poisson noise [23] was added to the LED based Raman spectra, which were synthesized by the configuration of 10nm bandwidth LED, to further test the robustness of the proposed method. The signal-to-ratio of the noisy LED based Raman spectra are approximately 40. By using those noisy LED based Raman spectra as the input of the proposed method, it can be found that the differences between the narrow-band measurements of noisy LED based Raman spectra and those of LED based Raman spectra without noise are always less than 1.5%. This is attributed to the fact that the narrow-band measurements are the intensity integration

TABLE 4. The comparison of the mean relative RMSEs for the results of LED based Raman measurements without noise and the results of noisy LED based Raman measurements.

	Phantom	Blood serum	Cell
LED based Raman spectra without noise	5.81×10^{-3}	1.22×10^{-2}	1.67×10^{-2}
Noisy LED based Raman spectra	5.82×10^{-3}	1.22×10^{-2}	1.68×10^{-2}

along the wavelength dimension, in which a large proportion of shot noise can be removed during such integration [22]. Furthermore, by using the same number of non-negative PCs based filters, only negligible degradation of the mean relative RMSEs can be found between the results of noisy LED based Raman spectra and the results for LED based Raman spectra without noise, as shown in Table 4. We believe that the results can be even closer when the de-noising preprocessing is employed.

According to the above results, it has been demonstrated that high spectral resolution Raman measurements can be achieved when using LED as excitation based on the proposed weighted spectral reconstruction method, in which the mean relative RMSEs can be less than 2% in all types of sample investigated in this study and even the worst relative RMSEs for each test sample can be less than 6%. In addition, the LED bandwidth, number of non-negative PCs based filters and the complexity of the Raman spectral shape show significant impact on the spectral reconstruction accuracy, which is the same as we expected, thus the optimal configurations for Raman spectra from different types of samples is with significant importance, especially for the choice of LEDs bandwidth. Although the proposed method is a supervised learning method in nature and requires training dataset, the proposed method can still work in many biomedical applications, in which building the training dataset is uncomplicated and the unexpected samples rarely exist. Compared to the previous studies that use complex instruments to improve the spectral resolution of the collected Raman measurements,

the proposed method provides the possibility of performing Raman measurements in a simple and cost-effective Raman setup without considerably sacrificing the quality of Raman measurements, and the spectral resolution is even close to the conventional Raman measurements. It should be noted that the filter characteristic can play an important role on the spectral reconstruction accuracy. However, in this study, the LED based Raman measurements can be collected with a conventional spectroscopy system, and the narrow-band measurement can be numerically calculated by the inner product of the LED based Raman spectrum and the optimized transmittance, thus real filters are not necessary and non-perfect transmittance can be avoided. Real filters are only required when the LED based Raman spectroscopy is further simplified to collect Raman spectrum by a single channel detector or modified to a Raman imaging system, in which LED based narrow-band measurements can be captured by a single channel detector for Raman spectroscopy or from a field of view for Raman imaging. Although those filters are typically with complex transmittance, they can be fabricated by the programmable optical filter and the transmittance can be finely calibrated by a Hadamard transform based calibration method as in the published paper [24].

V. CONCLUSION

In this study, a weighted spectral reconstruction method was developed and theoretically evaluated to retrieve high spectral resolution Raman spectra from the Raman measurements using LED as the excitation. Furthermore, the impact factor related to final spectral reconstruction accuracies were investigated and summarized, such as the LED bandwidth, number of non-negative PCs based filters, and the Raman spectral complexity. The results demonstrate that the reconstructed Raman spectra from LED based Raman measurements based on the proposed method are in excellent agreement with the conventional laser based Raman measurements. Considering the advantages of using LED instead of narrow-band laser, the methods described in this paper can be applicable to a portable and cost-effective LED based Raman spectroscopy system or even LED based Raman spectroscopic imaging setup.

REFERENCES

[1] C. V. Raman and K. S. Krishnan, "A new type of secondary radiation," *Nature*, vol. 121, no. 3048, pp. 501–502, 1928.
[2] L. Chen, "Near-infrared confocal micro-Raman spectroscopy combined with PCA–LDA multivariate analysis for detection of esophageal cancer," *Laser Phys.*, vol. 23, no. 6, Apr. 2013, Art. no. 065601.
[3] X. Zhang, Q.-H. Tan, J.-B. Wu, W. Shi, and P.-H. Tan, "Review on the Raman spectroscopy of different types of layered materials," *Nanoscale*, vol. 8, no. 12, pp. 6435–6450, 2016.
[4] K. Kneipp, H. Kneipp, I. Itzkan, R. R. Dasari, and M. S. Feld, "Ultrasensitive chemical analysis by Raman spectroscopy," *Chem. Rev.*, vol. 99, no. 10, pp. 2957–2976, Oct. 1999.
[5] J. Jehlička and H. G. M. Edwards, "Raman spectroscopy as a tool for the non-destructive identification of organic minerals in the geological record," *Organic Geochem.*, vol. 39, no. 4, pp. 371–386, Apr. 2008.
[6] C. Krafft, B. Dietzek, and J. Popp, "Raman and CARS microspectroscopy of cells and tissues," *Analyst*, vol. 134, no. 6, pp. 1046–1057, Jul. 2009.
[7] I. Nabiev, I. Chourpa, and M. Manfait, "Applications of Raman and surface-enhanced Raman scattering spectroscopy in medicine," *J. Raman Spectrosc.*, vol. 25, no. 1, pp. 13–23, Jan. 1994.
[8] T. Mu, S. Li, H. Feng, C. Zhang, B. Wang, X. Ma, J. Guo, B. Huang, and L. Zhu, "High-sensitive smartphone-based Raman system based on cloud network architecture," *IEEE J. Sel. Topics Quantum Electron.*, vol. 25, no. 1, Jan./Feb. 2018, Art. no. 7200306.
[9] M. A. Schmidt and J. Kiefer, "Polarization-resolved high-resolution Raman spectroscopy with a light-emitting diode," *J. Raman Spectrosc.*, vol. 44, no. 11, pp. 1625–1627, Nov. 2013.
[10] R. Adami and J. Kiefer, "Light-emitting diode based shifted-excitation Raman difference spectroscopy (LED-SERDS)," *Analyst*, vol. 138, no. 21, pp. 6258–6261, Sep. 2013.
[11] J. S. Greer, G. I. Petrov, and V. V. Yakovlev, "Raman spectroscopy with LED excitation source," *J. Raman Spectrosc.*, vol. 44, no. 7, pp. 1058–1059, Jul. 2013.
[12] S. Chen, L. Kong, W. Xu, X. Cui, and Q. Liu, "A fast fluorescence background suppression method for Raman spectroscopy based on stepwise spectral reconstruction," *IEEE Access*, vol. 6, pp. 67709–67717, 2018.
[13] D. Wei, S. Chen, Y. H. Ong, C. Perlaki, and Q. Liu, "Fast wide-field Raman spectroscopic imaging based on simultaneous multi-channel image acquisition and Wiener estimation," *Opt. let.*, vol. 41, no. 12, pp. 2783–2786, Jun. 2016.
[14] S. Chen, G. Wang, X. Cui, and Q. Liu, "Stepwise method based on Wiener estimation for spectral reconstruction in spectroscopic Raman imaging," *Opt. Express*, vol. 25, no. 2, pp. 1005–1018, Jan. 2017.
[15] S. Chen, Y. H. Ong, and Q. Liu, "A method to create a universal calibration dataset for Raman reconstruction based on wiener estimation," *IEEE J. Sel. Topics Quantum Electron.*, vol. 22, no. 3, pp. 164–170, May/Jun. 2016.
[16] S. Chen, Y. H. Ong, and Q. Liu, "Fast reconstruction of Raman spectra from narrow-band measurements based on Wiener estimation," *J. Raman Spectrosc.*, vol. 44, no. 6, pp. 875–881, Jun. 2013.
[17] J. Zhao, M. M. Carrabba, and F. Allen, "Automated fluorescence rejection using shifted excitation Raman difference spectroscopy," *Appl. Spectrosc.*, vol. 56, no. 7, pp. 834–845, Jul. 2002.
[18] S. Chen, Y. H. Ong, X. Lin, and Q. Liu, "Optimization of advanced Wiener estimation methods for Raman reconstruction from narrow-band measurements in the presence of fluorescence background," *Biomed. Opt. Express*, vol. 6, no. 7, pp. 2633–2648, Jul. 2015.
[19] H. Haneishi, T. Hasegawa, A. Hosoi, Y. Yokoyama, N. Tsumura, and Y. Miyake, "System design for accurately estimating the spectral reflectance of art paintings," *Appl. Opt.*, vol. 39, no. 35, pp. 6621–6632, Dec. 2000.
[20] S. Chen and Q. Liu, "Modified Wiener estimation of diffuse reflectance spectra from RGB values by the synthesis of new colors for tissue measurements," *J. Biomed. Opt.*, vol. 17, no. 3, Mar. 2012, Art. no. 030501.
[21] R. Piché, "Nonnegative color spectrum analysis filters from principal component analysis characteristic spectra," *J. Opt. Soc. Amer. A, Opt. Image Sci.*, vol. 19, no. 10, pp. 1946–1950, Oct. 2002.
[22] S. Chen, X. Lin, C. Yuen, S. Padmanabhan, R. W. Beuerman, and Q. Liu, "Recovery of Raman spectra with low signal-to-noise ratio using Wiener estimation," *Opt. Express*, vol. 22, no. 10, pp. 12102–12114, May 2014.
[23] D. Van de Sompel, E. Garai, C. Zavaleta, and S. S. Gambhir, "A comparison of noise models in a hybrid reference spectrum and principal components analysis algorithm for Raman spectroscopy," *J. Raman Spectrosc.*, vol. 44, no. 6, pp. 841–856, May 2013.
[24] J. Kang, X. Li, and Q. Liu, "Hadamard transform-based calibration method for programmable optical filters based on digital micro-mirror device," *Opt. Express*, vol. 26, no. 15, pp. 19563–19573, Jul. 2018.

SHUO CHEN received the bachelor's degree from Shanghai Jiaotong University, China, the master's degree from Heidelberg University, Germany, and the Ph.D. degree from the School of Chemical and Biomedical Engineering, Nanyang Technological University, Singapore. He is currently an Associate Professor with the College of Medicine and Biological Information Engineering, Northeastern University, China. His research interest includes fast spectroscopic imaging in biomedical applications.

MIXING LIU received the bachelor's degree from Nanchang Hangkong University, China. She is currently pursuing the master's degree with the College of Medicine and Biological Information Engineering, Northeastern University, China. Her research interest includes spectroscopic imaging in biomedical applications.

JING LIU received the bachelor's degree from Zhejiang University, China, and the master's degree from the Graduate School of the Second Academy of China Aerospace. She is currently an Assistant Engineer with the Science and Technology on Optical Radiation Laboratory, Beijing Institute of Environmental Features. Her research interests include infrared remote sensing detection and data processing and analysis.

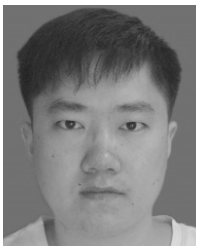

LINGMIN KONG received the bachelor's degree in automation from the Taiyuan University of Technology, China, and the master's degree in biomedical engineering from Northeastern University, China. His research interest includes fast spectroscopic imaging in biomedical applications.

WENBIN XU received the Ph.D. degree in optical engineering from the University of Chinese Academy of Sciences. He is currently a Senior Engineer with the Science and Technology on Optical Radiation Laboratory, Beijing Institute of Environmental Features. His research interests include infrared spectroscopy and spectral data processing in industrial applications.

GANG HOU received the bachelor's degree from the Shenyang Medical College, the master's and M.D. degrees from China Medical University. He is currently a Professor with The First Hospital of China Medical University. His research interests include interventional pulmonology, chronic airway disease, and interstitial lung disease.

LIPING XIE received the bachelor's and master's degrees from Jilin University, China, in 2008 and 2010, respectively, and the Ph.D. degree from Tsinghua University, China, in 2014. She is currently with Northeastern University. Her research interests include stretchable electronic materials, and devices and biosensing.

XIAOYU CUI received the bachelor's degree from the Shenyang University of Technology, China, and the master's and Ph.D. degrees in biomedical engineering from Northeastern University, China, where he is currently an Associate Professor with the College of Medicine and Biological Information Engineering. His research interests include optical imaging and machine learning in biomedical applications.